ELSEVIER

Data Article

Dataset of wind setup in a regulated Venice lagoon

Check for updates

Riccardo Mel[*], Luca Carniello, Luigi D'Alpaos

Dipartimento di Ingegneria Civile, Edile e Ambientale (ICEA), Università degli Studi di Padova, Italy

A B S T R A C T

This data article includes the dataset of wind setup in the Venice lagoon computed by means of a 2-D hydrodynamic model. The capability of the model to reproduce the hydrodynamic regime of the lagoon has been extensively investigated, with particular attention to the calibration of the wind shear stress at the water surface, in order to precisely characterize the contribute of wind setup on the water level estimation inside the lagoon.

We analyze the wind setup induced considering all the reliable wind speeds (with step of 1 m/s) and wind directions (with step of 30°) potentially blowing over the Venice lagoon, comparing the results obtained considering the present not-regulated configuration of the lagoon (pre-Mo.S.E. scenario) to the regulated configuration (post-Mo.S.E. scenario), which refers to the hydrodynamic regime when the Mo.S.E. movable barriers will be operational. The analysis shows that the wind setup significantly increases when the gates at the three inlets of the Venice lagoon are regulated, up to exceeding four times the pre-Mo.S.E. scenario. We deem this result is of paramount importance for the management of the Mo.S.E. barriers and for the definition of their operating strategy aiming at preventing the flooding at all the urban settlements of the lagoon.

Specifications Table

Subject	Atmospheric Science, Earth-Surface Processes, Oceanography
Specific subject area	Hydrodynamics and wind setup of the Venice lagoon, Mo.S.E. system management
Type of data	Table
	Chart
	Graph
	Figure
How data were acquired	Properly calibrated 2-D numerical model of the Venice lagoon
Data format	Raw
Parameters for data collection	Numerical simulations have been carried out on a computational grid representing the Venice lagoon based on the most recent and accurate bathymetric surveys
Description of data collection	We forced the model by imposing the wind field blowing over the lagoon and the tide at the three inlets
Data source location	Venice lagoon, Italy
Data accessibility	With the article
Related research article	Mel, R., Carniello L., D'Alpaos, L.
	Addressing the effect of the Mo.S.E. barriers closure on wind setup within the Venice lagoon
	Estuarine, Coastal and Shelf Science https://doi.org/10.1016/j.ecss.2019.106249

Value of the data

- The data can be useful for the optimization of the Mo.S.E. barriers management
- Any researcher that deals with the Venice lagoon can benefit from these dataset
- The data can be useful for further researches that deal with any regulated lagoon
- Wind setup in the Venice lagoon strongly depends on the regulation of the inlet gates
- The data investigate extensively the effect of the regulation of the inlet gates on the Venice lagoon hydrodynamics (post-Mo.S.E. scenario)
- The dataset includes the wind setup for any wind direction (step of 30°) and wind speed (step of 1 m/s) computed in both the pre-Mo.S.E. and post-Mo.S.E. scenario

1. Data

An accurate and reliable sea level (SL) forecast system is of paramount importance in defining the optimum operating strategy to face the emergency due to flood hazards that threat the urban
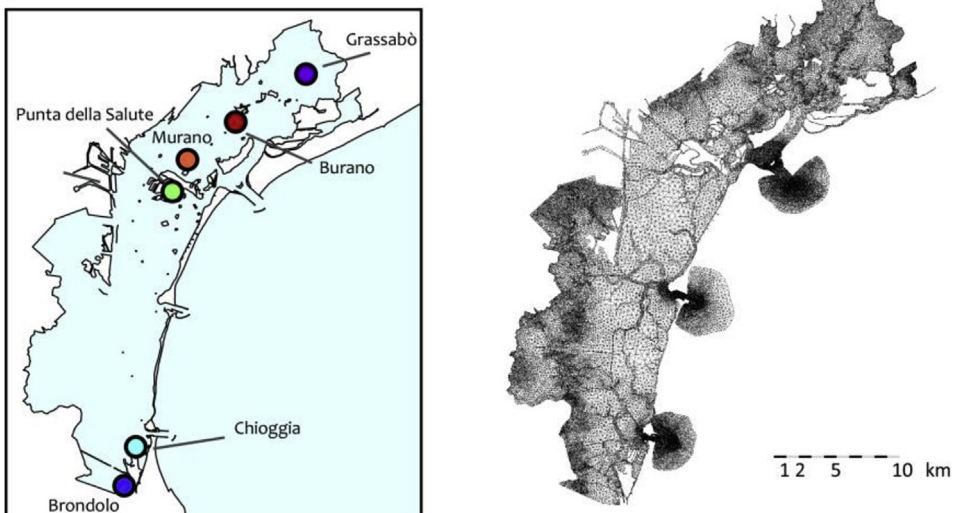

Fig. 1. Left panel shows the six CPSM lagoonal gauges where we computed the wind setup in both the pre-Mo.S.E. and post-Mo.S.E. scenario for any wind speed and wind direction (see the results in Figs. 2–4). Right panel shows the grid of the hydrodynamic model we used in the present analysis.
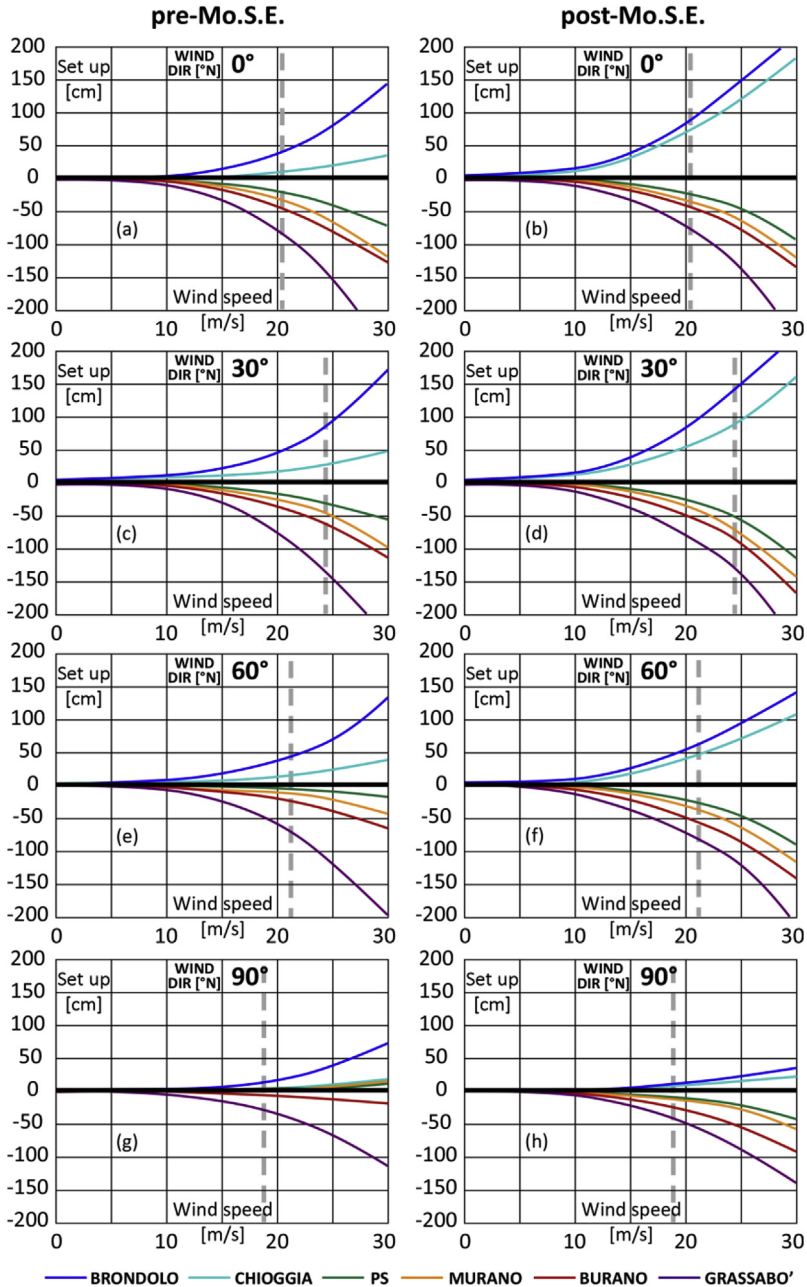
Fig. 2. North − Eastern winds complete analysis: relationship between wind setup and wind speed computed at the six CPSM gauges (Fig. 1). Vertical grey dashed lines represent the maximum wind speed recorded in the period 1999–2018 for that specific direction from which it originates. Left panels represent the pre-Mo.S.E. scenario (panel (a) for wind direction of 0°N, panel (c) for wind direction of 30°N, which has been already presented in the research article [8], panel (e) for wind direction of 60°N and panel (g) for wind direction of 90°N). Right panels represent the post-Mo.S.E. scenario for the same wind directions (panel (b) for wind direction of 0°N, panel (d) for wind direction of 30°N, which has been already presented in the research article [8], panel (f) for wind direction of 60°N and panel (h) for wind direction of 90°N).
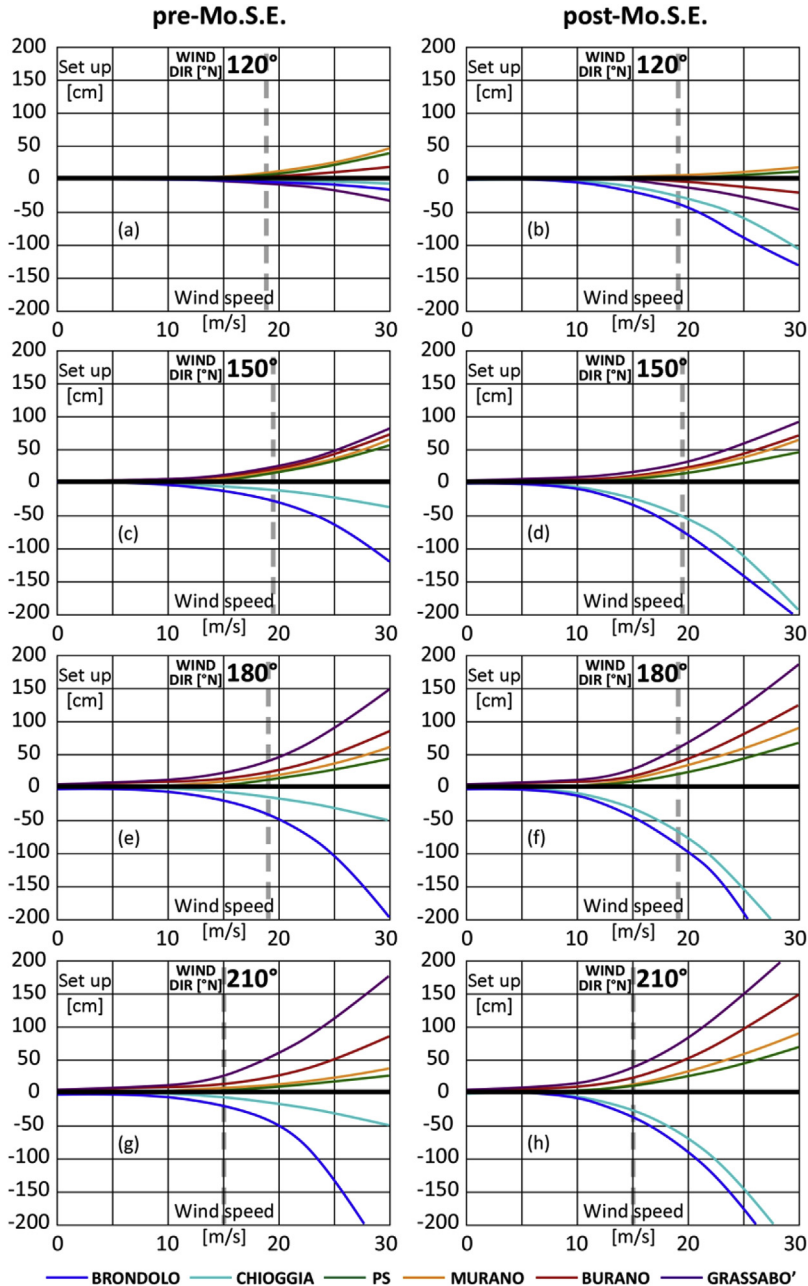
Fig. 3. Southern winds complete analysis: relationship between wind setup and wind speed computed at the six CPSM gauges (Fig. 1). Vertical grey dashed lines represent the maximum wind speed recorded in the period 1999−2018 for that specific direction. Left panels represent the pre-Mo.S.E. scenario (panel (a) for wind direction of 120°N, panel (c) for wind direction of 150°N, panel (e) for wind direction of 180°N, which has been already presented in the research article [8], and panel (g) for wind direction of 210°N). Right panels represent the post-Mo.S.E. scenario for the same wind directions (panel (b) for wind direction of 120°N, panel (d) for wind direction of 150°N, panel (f) for wind direction of 180°N, which has been already presented in the research article [8], and panel (h) for wind direction of 210°N).
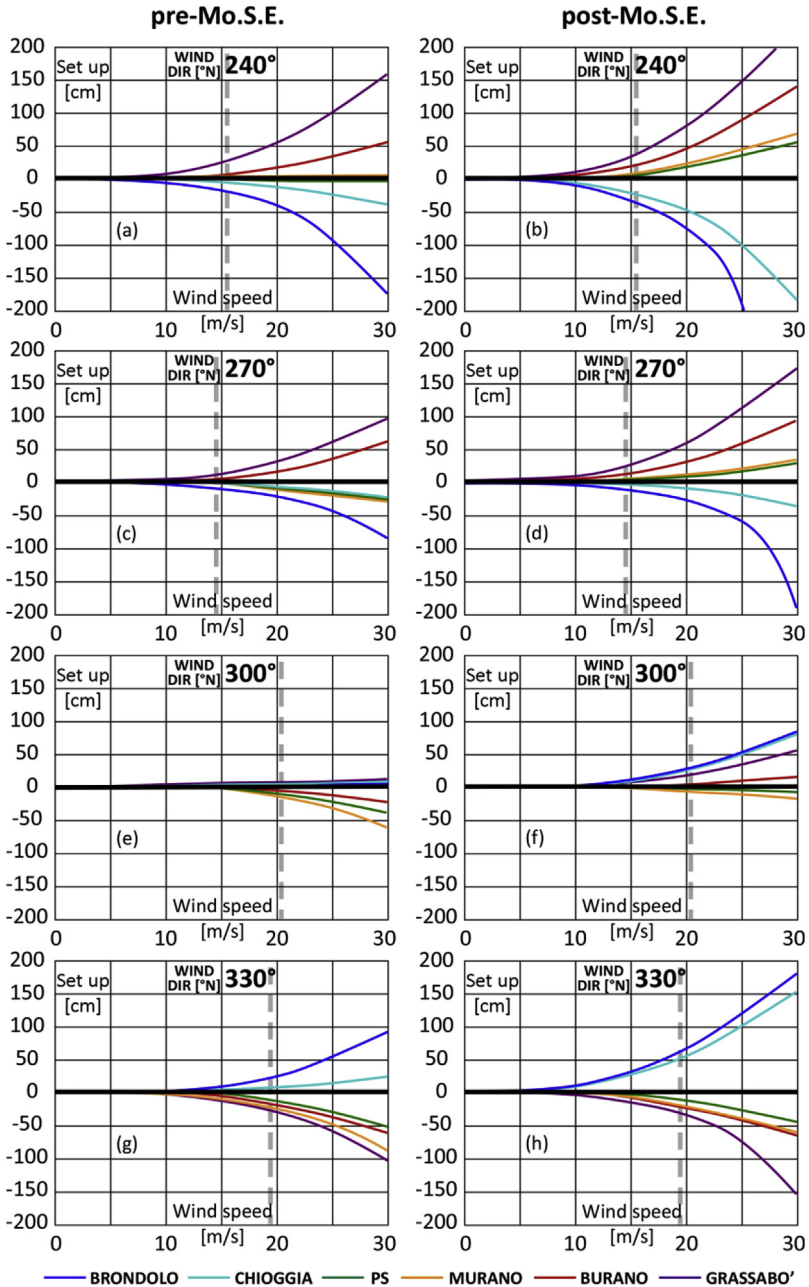
Fig. 4. North - Western winds complete analysis: relationship between wind setup and wind speed computed at the six CPSM gauges (Fig. 1). Vertical grey dashed lines represent the maximum wind speed recorded in the period 1999–2018 for that specific direction. Left panels represent the pre-Mo.S.E. scenario (panel (a) for wind direction of 240°N, panel (c) for wind direction of 270°N, panel (e) for wind direction of 300°N and panel (g) for wind direction of 330°N). Right panels represent the post-Mo.S.E. scenario for the same wind directions (panel (b) for wind direction of 240°N, panel (d) for wind direction of 270°N, panel (f) for wind direction of 300°N and panel (h) for wind direction of 330°N).

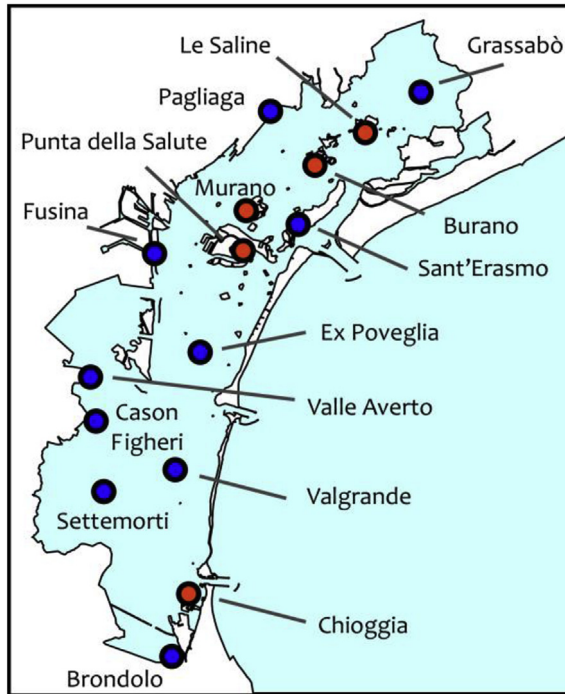**Fig. 5.** The 15 lagoonal gauges where the capability of the model to reproduce wind setup has been calibrated (the 5 gauges represented with red bullets) and tested (all the 15 gauges of the panel) by means of three conventional statistic parameters: the Nash Sutcliffe Model Efficiency (NSE), the Percentage Model Bias (PB) and the Scatter Index (SI).

settlements located in the Venice lagoon [7]. The data we present and discuss in the present contribution are related to the research article "Addressing the effect of the Mo.S.E. barriers closure on wind setup within the Venice lagoon" [8].

The dataset consists in the SL gradient and the wind setup we obtained using a 2D hydrodynamic model considering any direction and speed of the wind potentially blowing over the Venice lagoon. In performing such a systematic analysis, we compare the water levels obtained considering both the pre-Mo.S.E. (open inlets) and the post-Mo.S.E. (inlets regulated by the presence of the movable gates) scenario at six locations within the lagoon. These locations correspond to six stations of the Centro Previsioni e Segnalazioni Maree (CPSM) monitoring network and are located at: Brondolo (extreme South of the lagoon), Chioggia town (penalized by North-eastern winds), Punta della Salute (representing the SL for the city of Venice), Murano, Burano (penalized by Southern winds), and Grassabò (extreme North of the lagoon). The position of the gauges is shown in Fig. 1, while the results are summarized in Fig. 2, Fig. 3 and Fig. 4.

Figs. 2–4 provide the effect of the wind setup (i.e. the difference between the SL at the end of each run and the initial uniform SL - see the following chapter for the description of the characteristics of the simulations) for all the wind speeds and all the wind directions at the six CPSM monitoring stations. Results for intermediate directions can be obtained via linear interpolation without a significant difference (lower than 2%). Panels (a), (c), (e) and (g) of Figs. 2–4 refer to the pre-Mo.S.E. scenario, while panels (b), (d), (f) and (h) to the post-Mo.S.E. scenario. Results concerning wind directions of 30°N and 180°N (Fig. 1 panels (c) - (d) and Fig. 2 panels (e) - (f) respectively) have been already presented and discussed in the research paper [8].
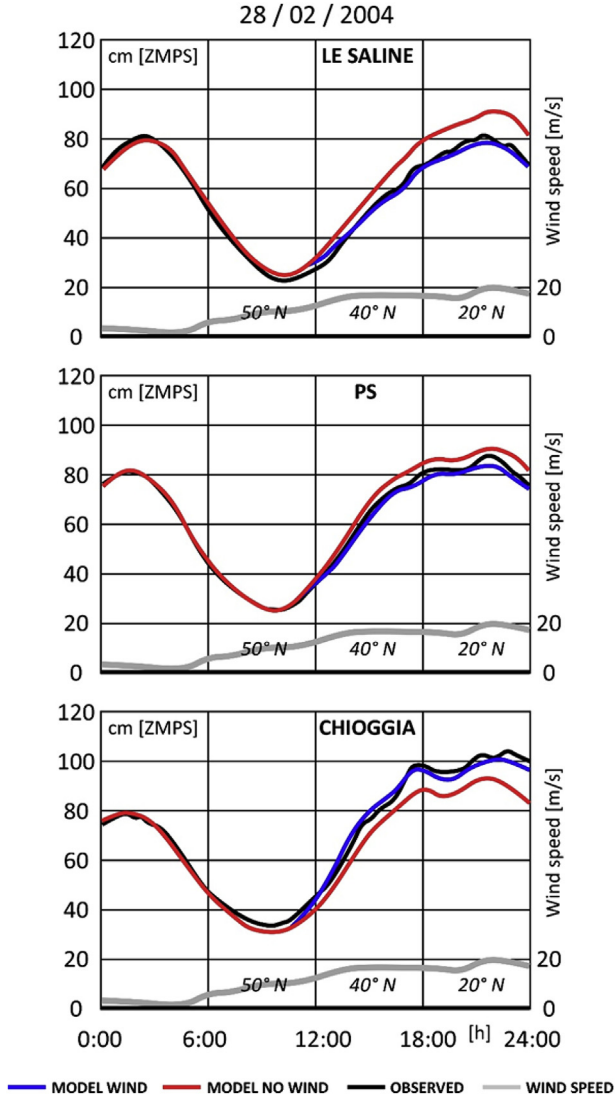
Fig. 6. Example of the model capability to reproduce the wind setup: storm surge occurred on February 28th, 2004. Comparison between the SLs computed by the model (blue lines) with those measured (black lines) at three representative stations of Fig. 5, namely: Le Saline in the Northern lagoon, Punta della Salute and Chioggia in the South. Red lines represent the SLs computed by the model neglecting the wind effect.

2. Experimental design, materials, and methods

Wind setup have been computed by means of a coupled wind wave-tidal model (WWTM, see [2,4]). A preliminary but fundamental part of this work consists in a further calibration the model, with particular attention to the wind shear stress at the water surface (τ_{wind}), in order to precisely determine the contribute of wind setup on the SL estimation. The WWTM estimates τ_{wind} as:

$$\tau_{wind} = \rho c_d \left(1 - e^{e_w U_{wind}} \right) U_{wind}^2 \tag{1}$$

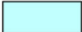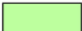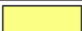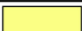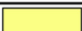|	Index value	Performance	Cell colour
NSE	> 0.65	Excellent	
	0.65 - 0.50	Very good	
	0.50 - 0.20	Good	
	< 0.20	Fair	
PB	< 10	Excellent	
	10 - 20	Very good	
	20 - 40	Good	
	> 40	Fair	
SI	< 0.3	Excellent	
	0.3 - 0.5	Very good	
	0.5 - 1	Good	
	> 1	Fair	

Fig. 7. The four performance ranges of the three parameters used in the performance test of the model. Results are shown in Figs. 8−10.

NSE$_{WIND}$ Index																		
Data	**h**	**WD [°N]**	**WV [m/s]**	**PS**	**MUR**	**CHI**	**BUR**	**SAL**	**GRA**	**PAG**	**SER**	**FUS**	**BRO**	**SET**	**VAL**	**EXP**	**FIG**	**AVE**
6/11/2000	19	145	18	0.67	#N/D	0.65	#N/D	#N/D	0.95	#N/D	0.77	0.51	0.78	N/S	N/S	0.65	#N/D	#N/D
16/11/2002	14	125	12	0.93	#N/D	N/S	#N/D	N/S	0.80	0.90	N/S	0.85	N/S	N/S	N/S	N/S	0.87	0.90
24/9/2004	18	50	24	N/S	N/S	N/S	#N/D	0.89	0.81	0.48	0.72	0.70	#N/D	N/S	N/S	N/S	0.68	0.25
3/12/2005	12	165	12	0.89	0.91	0.81	0.51	0.53	#N/D	0.91	0.68	0.74	0.92	N/S	N/S	N/S	N/S	N/S
19/3/2007	10	205	13	N/S	N/S	0.88	0.38	0.75	0.64	#N/D	0.86	N/S	0.88	N/S	N/S	N/S	N/S	N/S
14/9/2008	14	35	16	0.64	0.59	0.88	0.89	0.71	0.69	0.90	0.81	N/S	#N/D	0.89	0.89	N/S	0.77	0.82
28/11/2008	16	30	18	0.82	0.82	0.67	0.49	0.47	0.23	0.68	0.59	N/S	0.53	0.90	0.79	N/S	0.36	0.25
26/12/2008	5	60	18	0.69	0.90	0.60	0.96	0.67	0.75	0.78	0.90	N/S	0.77	0.90	0.85	N/S	0.79	0.77
9/3/2010	7	45	23	0.25	#N/D	0.75	0.79	0.88	#N/D	#N/D	#N/D	#N/D	#N/D	#N/D	#N/D	#N/D	#N/D	#N/D
1/11/2012	1	40	16	0.65	#N/D	0.45	0.98	0.99	#N/D	#N/D	#N/D	#N/D	#N/D	#N/D	#N/D	#N/D	#N/D	#N/D
11/11/2012	12	140	15	0.77	#N/D	0.24	0.73	0.29	#N/D	#N/D	#N/D	#N/D	#N/D	#N/D	#N/D	#N/D	#N/D	#N/D

Fig. 8. Model capability of reproducing the wind setup estimated by the Nash Sutcliffe Model Efficiency (NSE) comparing the computed and measured SLs at the 15 stations represented in Fig. 5. #N/D stands for no data and #N/S for not significant wind setup (less than 5 cm).

PB$_{WIND}$ Index																		
Data	h	WD [°N]	WV [m/s]	PS	MUR	CHI	BUR	SAL	GRA	PAG	SER	FUS	BRO	SET	VAL	EXP	FIG	AVE
6/11/2000	19	145	18	6.2	#N/D	11.8	#N/D	#N/D	3.8	#N/D	8.7	7.7	5.6	N/S	N/S	8.3	#N/D	#N/D
16/11/2002	14	125	12	5.2	#N/D	N/S	#N/D	N/S	21.4	2.7	N/S	2.1	N/S	N/S	N/S	N/S	8.9	5.7
24/9/2004	18	50	24	N/S	N/S	N/S	#N/D	4.3	5.5	16.1	6.6	13.3	#N/D	N/S	N/S	N/S	12.7	16.1
3/12/2005	12	165	12	2.9	3.1	8.9	19.3	20.7	#N/D	5.9	13.8	12.2	2.3	N/S	N/S	N/S	N/S	N/S
19/3/2007	10	205	13	N/S	N/S	16.4	28.3	19.9	19.8	#N/D	9.5	N/S	2.8	N/S	N/S	N/S	N/S	N/S
14/9/2008	14	35	16	18.1	19.6	5.0	2.0	5.6	5.0	4.2	9.8	N/S	#N/D	4.7	3.0	N/S	9.3	10.4
28/11/2008	16	30	18	9.7	8.8	14.7	7.8	14.2	26.4	11.8	9.9	N/S	28.7	4.1	0.8	N/S	14.2	11.9
26/12/2008	5	60	18	10.0	5.6	8.4	1.7	14.9	7.7	2.8	8.3	N/S	6.0	3.4	3.6	N/S	10.9	8.6
9/3/2010	7	45	23	10.5	#N/D	2.9	3.5	1.9	#N/D	#N/D	#N/D	#N/D	#N/D	#N/D	#N/D	#N/D	#N/D	#N/D
1/11/2012	1	40	16	9.7	#N/D	19.8	1.5	0.3	#N/D	#N/D	#N/D	#N/D	#N/D	#N/D	#N/D	#N/D	#N/D	#N/D
11/11/2012	12	140	15	7.1	#N/D	24.6	14.4	29.4	#N/D	#N/D	#N/D	#N/D	#N/D	#N/D	#N/D	#N/D	#N/D	#N/D

Fig. 9. Model performance estimated by the Percentage Model Bias (PB), comparing the computed and measured SLs at the 15 stations represented in Fig. 5. #N/D stands for no data and #N/S for not significant wind setup (less than 5 cm).

SI$_{WIND}$ Index																		
Data	h	WD [°N]	WV [m/s]	PS	MUR	CHI	BUR	SAL	GRA	PAG	SER	FUS	BRO	SET	VAL	EXP	FIG	AVE
6/11/2000	19	145	18	0.12	#N/D	0.23	#N/D	#N/D	0.20	#N/D	0.24	0.12	0.25	N/S	N/S	0.16	#N/D	#N/D
16/11/2002	14	125	12	0.12	#N/D	N/S	#N/D	N/S	0.37	0.32	N/S	0.07	N/S	N/S	N/S	N/S	0.14	0.13
24/9/2004	18	50	24	N/S	N/S	N/S	#N/D	0.02	0.10	0.28	0.17	0.42	#N/D	N/S	N/S	N/S	0.26	0.39
3/12/2005	12	165	12	0.05	0.10	0.21	0.27	0.28	#N/D	0.44	0.51	0.25	0.12	N/S	N/S	N/S	N/S	N/S
19/3/2007	10	205	13	N/S	N/S	0.32	0.49	0.30	0.29	#N/D	0.27	N/S	0.20	N/S	N/S	N/S	N/S	N/S
14/9/2008	14	35	16	0.27	0.30	0.12	0.06	0.10	0.31	0.11	0.27	N/S	#N/D	0.06	0.06	N/S	0.41	0.25
28/11/2008	16	30	18	0.20	0.22	0.22	0.13	0.20	0.42	0.23	0.13	N/S	0.44	0.01	0.17	N/S	0.27	0.27
26/12/2008	5	60	18	0.17	0.12	0.13	0.04	0.21	0.12	0.05	0.15	N/S	0.21	0.08	0.45	N/S	0.14	0.27
9/3/2010	7	45	23	0.16	#N/D	0.07	0.06	0.02	#N/D	#N/D	#N/D	#N/D	#N/D	#N/D	#N/D	#N/D	#N/D	#N/D
1/11/2012	1	40	16	0.16	#N/D	0.27	0.03	0.01	#N/D	#N/D	#N/D	#N/D	#N/D	#N/D	#N/D	#N/D	#N/D	#N/D
11/11/2012	12	140	15	0.10	#N/D	0.38	0.24	0.47	#N/D	#N/D	#N/D	#N/D	#N/D	#N/D	#N/D	#N/D	#N/D	#N/D

Fig. 10. Model capability in reproducing the wind setup estimated by the Scatter Index (SI), comparing the computed and measured SLs at the 15 stations represented in Fig. 5. #N/D stands for no data and #N/S for not significant wind setup (less than 5 cm).

c_D	% OF SETUP
0.00	0
0.01	14
0.02	27
0.03	40
0.04	52
0.05	64
0.06	76
0.07	88
0.08	100
0.09	112
0.10	123
0.11	134
0.12	145
0.13	156
0.14	166
0.15	176
0.16	185

SL ICs, BCs	% OF SETUP
30	111
35	110
40	109
45	108
50	107
55	106
60	105
65	104
70	103
75	102
80	101
85	100
90	99
95	98
100	97
105	96
110	95

Ks	% OF SETUP
-10	95
-8	96
-6	97
-4	98
-2	99
CALIBRATED	100
+2	101
+4	102
+6	103
+8	104
+10	105

t WIND	% OF SETUP
0.5	12
1.0	36
1.5	55
2.0	70
2.5	80
3.0	87
3.5	91
4.0	94
4.5	96
5.0	97
5.5	98
6.0	99

Fig. 11. Sensitivity analysis of the model in computing the wind setup. Panels 1–4 show the percentage of the setup with respect to the values reported in Figs. 2–4. Panel 1 shows the results of the sensitivity analysis for the friction coefficient c_d (calibrated value 0.08). Panel 2 shows the results of the sensitivity analysis for the SL imposed at the three inlets (BCs) and the initial uniform water level of the lagoon (ICs). Panel 3 provides the effect on the estimated wind setup induced by variations of the Strickler coefficient with respect to the calibrated set of values. Panel 4 shows the relationship between the duration of the synthetic storm (i.e. constant wind speed and direction) and the percentage of the wind setup with respect to the value reached at equilibrium (i.e. considering a storm duration of 12 hours). As a representative example the results refer to the Chioggia station and to a Bora wind of 18 m/s. However, they do not significantly depend on the station and on wind direction and intensity.

where ρ is the water density, U_{wind} is the wind speed at 10 m and cd and e_w are calibration parameters. The numerical model has been already widely tested not only in the Venice lagoon (see [1–3,6]) but also in other microtidal lagoons worldwide (e.g. the lagoons of the Virginia Coast Reserve, USA [5], Cádiz Bay, Spain, [9]). All the same, we carried out a set of runs, reproducing some recent storm events characterized by different tidal and meteorological conditions, for calibrating c_d and e_w in eq. (1) and for further investigating the capability of the model in reproducing the lagoon hydrodynamics under stormy conditions. Toward this goal we selected 5 storm surges occurred between the 1999 and the 2018, all characterized by wind speed greater than 15 m/s and a SL peak recorded at Punta della Salute (PS) gauge station greater than 80 cm above the conventional reference datum of the PS station (ZMPS). We compared over the whole duration of the events the SLs computed by the model with those measured at 5 CPSM SL gauges (Le Saline, Burano, Murano, Punta della Salute and Chioggia, see Fig. 5, red bullets), almost uniformly distributed along the longitudinal axis of the lagoon at locations suitable for the analysis and estimation of the wind induced SL gradients. The most appropriate values of the calibration parameters for the estimation of the wind shear stress at the water surface ($c_d = 0.08$ and $e_w = 1.62\text{E-}06$ s/m) were estimated by minimizing the absolute SL rms error at the 5 CPSM gauges over the entire duration of the 5 storm events. An example is shown in Fig. 6 where we compare the time evolution of the computed and measured SL at three representative stations, namely: Le Saline, Punta della Salute and Chioggia, during the storm event occurred in February 28th, 2004.

We finally tested the model performance by comparing the computed and measured SLs at all the 15 lagoonal gauges of Fig. 5 and for 11 different storm surges characterized by Bora, Scirocco and Libeccio (blowing from South − West) winds. We used three conventional statistic parameters in order to evaluate the performance of the model in reproducing the wind setup: the Nash Sutcliffe Model Efficiency (NSE), the Percentage Model Bias (PB) and the Scatter Index (SI) (performance ranges are reported in Fig. 7). They measure respectively the ratio of model error and the variability in observational data (NSE), the model error normalized by the data (PB) and the rms error normalized with the mean of the observed data (SI). Results concerning all the three parameters (see Fig. 8, Fig. 9 and Fig. 10) indicate a very good performance of the model in estimating the wind setup (mean NSE = 0.72, mean PB = 9.8 and mean SI = 0.21). Absolute errors are generally comparable to measurement precision (2−3 cm).

Once calibrated and tested we used the numerical model for analyzing systematically the wind setup produced by all the possible wind directions and speeds. Toward this goal we run a set of 4320 numerical simulations, 2160 for the pre-Mo.S.E. scenario and 2160 for the post-Mo.S.E. scenario.

The characteristic of the simulations are the same we summarized in the research paper [8].

As ICs we imposed in the lagoon and at the three inlets a uniform SL equal to 85 cm ZMPS. As BCs we used:

   i) constant SL equal to 85 cm ZMPS at the three inlets;
  ii) constant and spatially uniform wind blowing over the whole surface of the lagoon for 12 hours;
 iii) wind direction varying form 0°N to 355°N with a step of 5°;
 iv) wind speed varying form 1 m/s to 30 m/s with a step of 1 m/s.

We further performed a sensitivity analysis concerning the initial conditions (ICs), the boundary conditions (BCs), the wind duration (t WIND), the bed roughness coefficient of the grid (Ks) and the friction coefficient (cd) used to compute the wind shear stress (Fig. 11, panels 1−4). In the sensitivity analysis we verified that:

   i) the SL, when forced by a constant and spatially uniform wind field, actually reaches the equilibrium in no more than 6 hours and almost the 90% of the wind setup is reached in less than 3 hours, a time comparable with the closure periods of the gates at the three inlets (Fig. 11, panel 4);
  ii) ICs do not affect the results we obtained for the wind setup inside the lagoon both in the pre-Mo.S.E. and in the post-Mo.S.E. scenario. Performing the sensitivity analysis using as ICs water levels inside the lagoon in the range 30−110 cm ZMPS, the maximum difference we obtained for the setup computed at all the considered monitoring stations is lower than 10%, with respect to the setup computed using 85 cm ZMPS as IC (Fig. 11, panel 2);
 iii) BCs imposed at the three inlets do not affect the results we obtained for the wind setup inside the lagoon in the pre-Mo.S.E. scenario. Performing the sensitivity analysis using as BCs values in the range 30−110 cm ZMPS the maximum difference we obtained for the setup computed at all the considered monitoring stations is again lower than 10%, with respect to the setup computed using 85 cm ZMPS as BC (Fig. 11, panel 2);
 iv) the Strickler bed roughness coefficient (Ks) used in the computational grid to describe the energy dissipation (Ks = 15 $m^{1/3}$/s for salt marshes, Ks = 20 $m^{1/3}$/s for tidal flats and Ks = 30 $m^{1/3}$/s for the main channels and the inlets) does not strongly affect the wind setup inside the lagoon. Performing a sensitivity analysis both increasing and decreasing the coefficient up to 10 $m^{1/3}$/s with respect to the calibrated values, the maximum difference we obtained for the wind setup computed at all the considered monitoring stations is lower than 5% (Fig. 11, panel 3).

Acknowledgments

Conflict of interest

The authors declare that they have no known competing financial interests or personal relationships that could have appeared to influence the work reported in this paper.

References

[1] L. Carniello, A. Defina, S. Fagherazzi, L. D'Alpaos, A combined wind wave-tidal model for the Venice lagoon, Italy, F04007, Journal of Geophysical Research − Earth Surface 110 (2005), https://doi.org/10.1029/2004JF000232. October 2005.

[2] L. Carniello, A. D'Alpaos, A. Defina, Modeling wind waves and tidal flows in shallow micro-tidal basins, Estuarine, Coastal and Shelf Science (2011), https://doi.org/10.1016/j.ecss.2011.01.001.

[3] L. D'Alpaos, A. Defina, Mathematical modeling of tidal hydrodynamics in shallow lagoons: a review of open issues and applications to the Venice lagoon, Comput. Geosci. (2006), https://doi.org/10.1016/j.cageo.2006.07.009.

[4] A. Defina, Two-dimensional shallow flow equations for partially dry areas, Water Resour. Res. 36 (11) (2000) 3251−3264.

[5] G. Mariotti, S. Fagherazzi, P. Wiberg, K. McGlathery, L. Carniello, A. Defina, Influence of storm surges and sea level on shallow tidal basin erosive processes, J. Geophys. Res. − Oceans 115 (2010) C11012, https://doi.org/10.1029/2009JC005892.

[6] R. Mel, D.P. Viero, L. Carniello, A. Defina, L. D'Alpaos, Simplified methods for real-time prediction of storm surge uncertainty: the city of Venice case study, Adv. Water Resour. 71 (2014a) 177−185, https://doi.org/10.1016/j.advwatres.2014.06.014.

[7] R. Mel, P. Lionello, Verification of an ensemble prediction system for storm surge forecast in the Adriatic Sea, Ocean Dyn. 64 (12) (2014b) 1803−1814.

[8] R. Mel, L. Carniello, L. D'Alpaos, Addressing the effect of the Mo.S.E. barriers closure on wind setup within the Venice lagoon, Estuarine, Coastal and Shelf Science 225 (2019). https://doi.org/10.1016/j.ecss.2019.106249.

[9] C. Zarzuelo, M. Diéz-Minguito, A. D'Alpaos, L. Carniello, J. Rosal-Salido, M. Ortega-Sánchez, Morphodynamic response to human activities in the bay of Cádiz (2012-2015), Coastal Engineering Proceedings, ICCE 2018 1−11 (2016), https://doi.org/10.9753/icce.v35 sediment.16.